Kinetics and Mechanism of Malonate Replacement in Bis(malonato)oxovanadate(IV) by Oxalate

JUNG-SUNG KIM

Department of Chemistry, Taegu University, Taegu, Korea

WOO-SIK JUNG, HIROSHI TOMIYASU and HIROSHI FUKUTOMI*

Research Laboratory for Nuclear Reactors, Tokyo Institute of Technology, O-okayama, Meguro-ku, Tokyo 152, Japan

(Received May 2, 1986; revised October 15, 1986)

Abstract

The kinetics of malonate replacement in bis-(malonato)oxovanadate(IV), $[VO(mal)_2H_2O]^{2-}$ (hereafter water molecule will be omitted), by oxalate has been studied by the stopped-flow method. The reaction was found to consist of two consecutive steps (k_1 and k_2: first-order rate constants) passing through a mixed ligand complex, $[VO(mal)(ox)]^{2-}$. The rates for each step depended linearly on the concentrations of free oxalate species, Hox^- and ox^{2-}. The second-order rate constants for the replacement by ox^{2-} were much larger in the k_1 step than in the k_2 step and the activation parameters were determined as follows: $\Delta H^{\neq} = 43.5 \pm 5.6$ kJ mol^{-1}, $\Delta S^{\neq} = -53 \pm 19$ J K^{-1} mol^{-1} and $\Delta H^{\neq} = 43.6 \pm 0.5$ kJ mol^{-1}, $\Delta S^{\neq} = -62 \pm 2$ J K^{-1} mol^{-1} for the k_1 and k_2 steps, respectively. The volume of activation was determined to be -0.65 ± 0.75 cm^3 mol^{-1} at 20.2 °C by the high-pressure stopped-flow method for the apparent rate constants.

Introduction

Despite a number of kinetic studies on ligand substitution reactions in oxovanadium(IV) complexes [1–15], kinetic behavior of bidentate ligands has not been well understood. In ligand exchange reactions between coordinated and free ligands in $[VOL_2]^{2-}$, where L = malonate (mal) [6] and oxalate (ox) [7], the rates were found to depend on the concentrations of free ligand species, L^{2-} and HL^-. On the other hand, the rates for replacement of glycinate in $VO(gly)_2$ (gly = glycinate) by oxalate were independent of the concentrations of free ligand [8]. It needs more kinetic results including activation volumes to further understand substitution mechanisms in oxovanadium(IV) complexes.

This paper presents the kinetic results of malonate replacement with oxalate

$$[VO(mal)_2]^{2-} + 2ox^{2-} \longrightarrow [VO(ox)_2]^{2-} + 2mal^{2-} \tag{1}$$
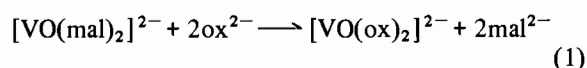
by means of the stopped-flow and high-pressure stopped-flow methods.

Experimental

An oxovanadium(IV) perchlorate solution was prepared by mixing stoichiometric amounts of oxovanadium(IV) sulfate and barium perchlorate (Wako Pure Chemical Ind., Ltd.) in aqueous solution, followed by the filtration of resulting barium sulfate. The concentration of VO^{2+} in solution was determined by titration with a standard $KMnO_4$ solution. Reagent grade malonic acid (Wako), sodium oxalate (Wako), and sodium perchlorate (Wako) were recrystallized twice from aqueous solutions before use. The ionic strength was adjusted to 1.0 M (M = mol dm^{-3}) by using sodium perchlorate. A Shimadzu UV-365 spectrophotometer was used for measurements of UV–Vis absorption spectra. The pH of solutions was measured with a Toa IM-20E pH meter. A Union Giken RA-401 stopped-flow spectrophotometer and a Hikari Kogaku FIT-3A high-pressure stopped-flow apparatus were used for kinetic measurements.

Results and Discussion

The solution of $[VO(mal)_2]^{2-}$, which was prepared in excess malonic acid, was stable and resistant to hydrolysis up to pH 6. In Fig. 1, the UV–Vis absorption spectrum of the above solution was the same as that of $[VO(mal)_2]^{2-}$ which was reported in the earlier paper [6]. Addition of excess Na_2ox gives a spectrum which was consistent with that of $[VO(ox)_2]^{2-}$ [7, 8]. Since $[VO(ox)_2]^{2-}$ was the only
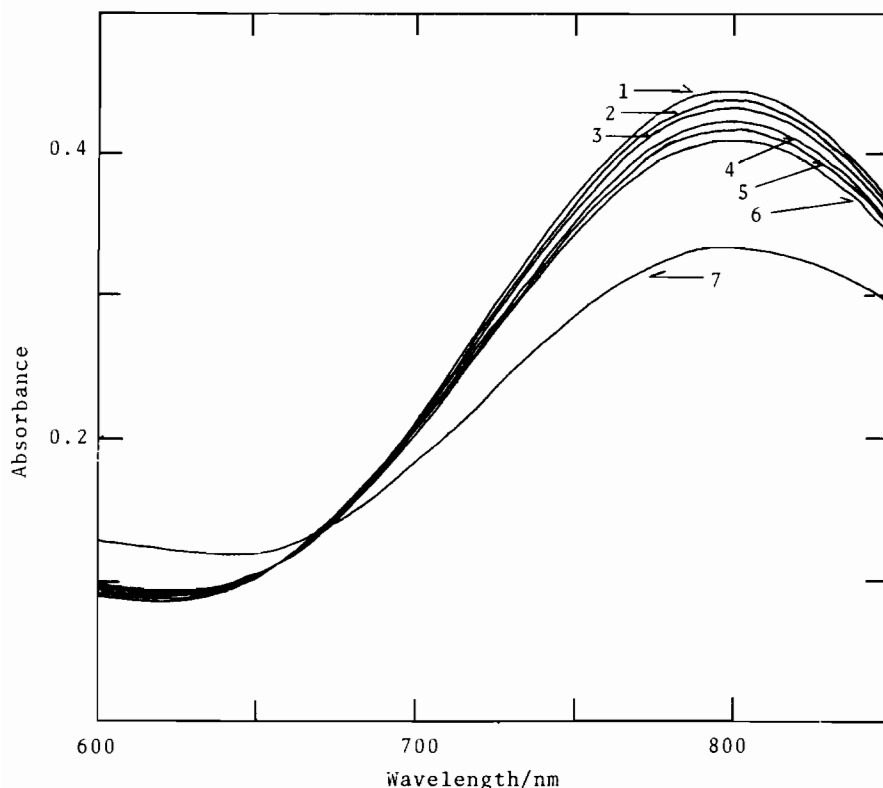
Fig. 1. Absorption spectrum of $[VO(mal)_2]^{2-}$ (1) and change in the spectrum by addition of small amount of Na_2ox (2–6). The conditions are as follows: $[VO^{2+}]_T = 0.0106$ M, $[H_2mal]_T = 1.00$ M; the pH of solutions was adjusted to 5.10 at 20 °C. Concentrations of added Na_2ox: 2, 0.00125; 3, 0.00250; 4, 0.00500; 5, 0.00750; 6, 0.0100 M. Spectrum (7) exhibits that of $[VO(ox)_2]^{2-}$. $[H_2ox]_T = 0.100$ M.
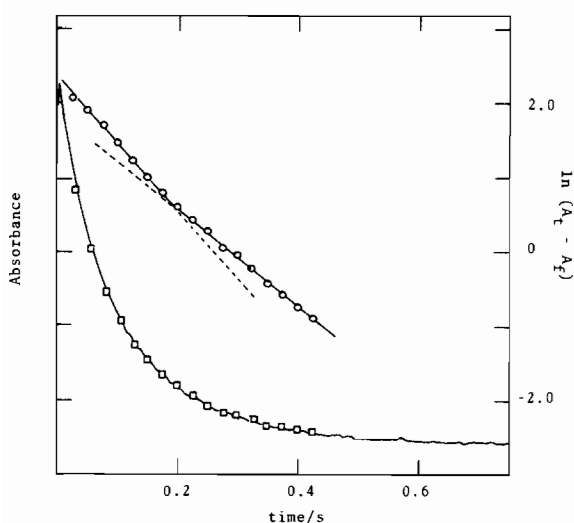

Fig. 2. A typical stopped-flow trace obtained under the following conditions: $[VO(mal)_2]^{2-} = 0.0107$ M, $[Na_2ox]_T = 0.100$ M, and pH = 5.32 at 23.8 °C. ○: pseudo-first-order plot; □: nonlinear least-squares fit based on eqn. (2). Measurements were carried out at 759 nm, where the best stopped-flow traces were obtained.

product of the reaction between $[VO(mal)_2]^{2-}$ and excess Na_2ox solutions, the stoichiometry can be written by eqn. (1).

Kinetic data were obtained from the change in absorbance at 759 nm by use of the stopped-flow apparatus. A typical stopped-flow trace is illustrated in Fig. 2 together with a pseudo-first-order plot $\ln(A_t - A_f)$ *versus* time, where A_t and A_f refer to the relative absorbances at times t and infinity, respectively. It can be seen in Fig. 2 that the pseudo-first-order plot deviates from a straight line suggesting that the reaction consists of two consecutive steps expressed by

$$[VO(mal)_2]^{2-} \xrightarrow{k_1} (Int) \xrightarrow{k_2} [VO(ox)_2]^{2-} \qquad (2)$$
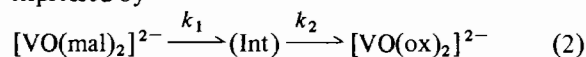
where k_1 and k_2 represent first-order rate constants and (Int) denotes an intermediate complex. The stopped-flow traces were analyzed by means of a nonlinear-least-squares method, where k_1, k_2 and the molar extinction coefficient of (Int), ϵ_{Int}, were used as unknown parameters to fit the following equation [17].

$$A_t - A_f = A \exp(-k_1 t) + B \exp(-k_2 t) \qquad (3)$$

where

$$A = \frac{(\epsilon_{Int} - \epsilon_A)k_1 + (\epsilon_A - \epsilon_C)k_2}{k_2 - k_1} \, [VO^{2+}]_T$$

$$B = \frac{(\epsilon_C - \epsilon_{Int})k_1}{k_2 - k_1} \, [VO^{2+}]_T$$

and ϵ_A and ϵ_C, molar extinction coefficients of $[VO(mal)_2]^{2-}$ and $[VO(ox)_2]^{2-}$, are 37 and 27 M^{-1} cm^{-1} at 759 nm, respectively, and $[VO^{2+}]_T$ refers to the total concentration of VO^{2+}. As is seen in Fig. 2, calculated values agree well with the observed trace giving the best-fit values for k_1, k_2 and ϵ_{Int}. Under the condition in Fig. 2, these values were determined as follows: $k_1 = 24.7$ s^{-1}, $k_2 = 7.48$ s^{-1}, and $\epsilon_{Int} = 31$ M^{-1} cm^{-1}.

It should be noted, however, that the mathematical analysis for such a consecutive reaction as eqn. (2) yields an alternative solution with a different set of parameters, k_1', k_2' and ϵ_{Int}' [17], where $k_1' = k_2$, $k_2' = k_1$ and

$$\epsilon_{Int}' = \epsilon_A + \frac{k_1(\epsilon_{Int} - \epsilon_A)}{k_2} \qquad (4)$$

The value of ϵ_{Int}' is calculated to be 17 M^{-1} cm^{-1}.

Additional experiments were carried out to estimate the approximate value of molar extinction coefficient of (Int) and to choose between ϵ_{Int} and ϵ_{Int}'. The change in the absorption spectrum of $[VO(mal)_2]^{2-}$ due to the addition of a small amount of Na_2ox is shown in Fig. 1. The spectra obtained in this way have an isosbestic point at 660 nm. Since the spectrum of $[VO(ox)_2]^{2-}$ does not pass through the above isosbestic point, the intermediate complex differs from $[VO(mal)_2]^{2-}$ and $[VO(ox)_2]^{2-}$ and it seems most likely that the intermediate is a mixed-ligand complex, $[VO(mal)(ox)]^{2-}$. The reaction can be written by
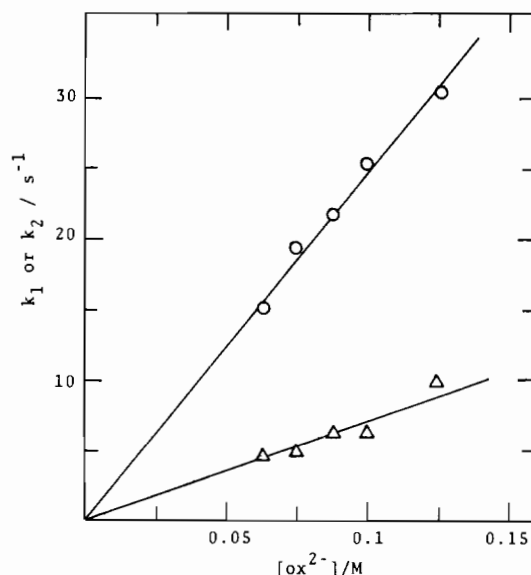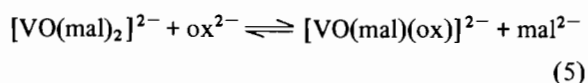
$$[VO(mal)_2]^{2-} + ox^{2-} \rightleftharpoons [VO(mal)(ox)]^{2-} + mal^{2-}$$

$$(5)$$

Fig. 3. Plots of k_1 or k_2 vs. $[ox^{2-}]$ at 23.8 °C. ○: k_1, △: k_2.

On the assumption that $[VO(mal)(ox)]^{2-}$ is formed stoichiometrically, the molar extinction coefficient of $[VO(mal)(ox)]^{2-}$ is calculated roughly to be 32 M^{-1} cm^{-1}. These results support the former solution for k_1 and k_2 with $\epsilon_{Int} = 31$ M^{-1} cm^{-1}.

The values of k_1 and k_2 were determined under a variety of conditions. The results obtained at pH 5.3–5.5 (Fig. 3), where ox^{2-} is the major species, reveals that both k_1 and k_2 are of first order in $[ox^{2-}]$ giving second-order rate constants as follows: $k_{1,ox} = 247$ M^{-1} s^{-1} and $k_{2,ox} = 74.7$ M^{-1} s^{-1} at 23.8 °C. The values of k_1 and k_2 obtained at various pH values are summarized in Table I. Both k_1 and k_2 are independent of pH in the high pH region (pH > 5.3), but increase as pH decreases below 5.0. This fact indicates that the rates are accelerated by hydrogenoxalate ion Hox^-, because $[Hox^-]$ exceeds 3% at pH below 5.0. These results lead to the following rate laws for k_1 and k_2

$$k_1 = k_{1,ox}[ox^{2-}] + k_{1,Hox}[Hox^-] \qquad (6a)$$

TABLE I. Observed Rate Constants for Malonate Replacement by Oxalate in $[VO(mal)_2]^{2-}$ at 20 °C at Various pH Values

pH	$[ox^{2-}]$ (M)[a]	$[Hox^-]$ (10^{-3} M)[a]	k_1 (s^{-1})	k_2 (s^{-1})
4.48	0.0895	10.5	40.3	7.55
4.73	0.0942	5.84	31.5	6.33
4.85	0.0952	4.77	29.7	6.38
5.00	0.0966	3.43	25.2	5.86
5.28	0.0982	1.83	20.9	5.59
5.68	0.0994	0.65	18.2	5.47
6.12	0.0997	0.27	19.1	5.69

[a] $[Na_2ox]_0 = 0.100$ M. The concentration of ox^{2-} and Hox^- were calculated by using values $pK = 3.55$ and $pK = 1.01$, respectively [16].
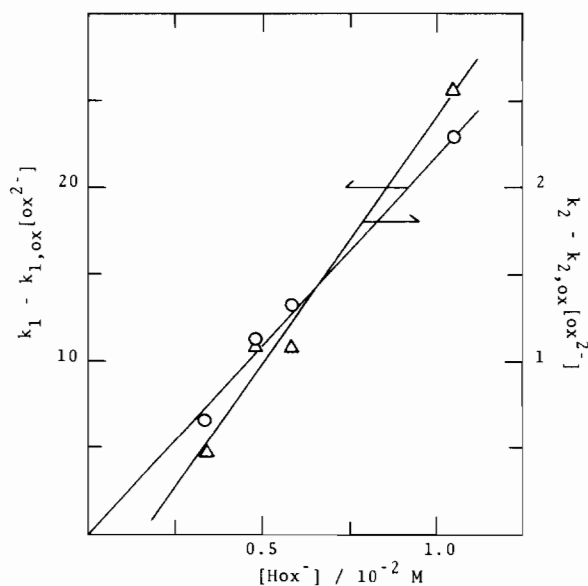
Fig. 4. Plots of $\{k_1 - k_{1,\text{ox}}[\text{ox}^{2-}]\}$ or $\{k_2 - k_{2,\text{ox}}[\text{ox}^{2-}]\}$ vs. $[\text{Hox}^-]$. $[\text{VO(mal)}_2]^{2-} = 0.0107$ M and $[\text{Na}_2\text{ox}]_\text{T} = 0.100$ M at 20 °C.

$$k_2 = k_{2,\text{ox}}[\text{ox}^{2-}] + k_{2,\text{Hox}}[\text{Hox}^-], \tag{6b}$$

where $k_{1,\text{ox}}$ and $k_{1,\text{Hox}}$, and $k_{2,\text{ox}}$ and $k_{2,\text{Hox}}$ refer to second-order rate constants for k_1 and k_2 with ox^{2-} and Hox^-, respectively. If eqns. (6a) and (6b) are correct, plots of $\{k_1 - k_{1,\text{ox}}[\text{ox}^{2-}]\}$ or $\{k_2 - k_{2,\text{ox}}[\text{ox}^{2-}]\}$ *versus* $[\text{Hox}^-]$ should give straight lines passing through the origin. As is shown in Fig. 4, the plot for k_1 is linear passing through the origin, and the plot for k_2 has a small intercept. However, considering relatively large errors in calculations, we assume that this intercept value is not significant and that eqn. (6b) is valid. The second-order rate constant with respect to Hox^-, $k_{1,\text{Hox}}$, is determined to be $(2.21 \pm 0.1) \times 10^3$ M^{-1} s^{-1} at 20 °C. The value for $k_{2,\text{Hox}}$ is roughly estimated to be 2.9×10^2 M^{-1} s^{-1} at 20 °C. It was also found that both k_1 and k_2 are independent of the total malonic acid concentration $[\text{H}_2\text{mal}]_\text{T}$ (Fig. 5).

From the results obtained at various temperatures (Table II) the activation parameters were determined for $k_{1,\text{ox}}$ and $k_{2,\text{ox}}$. The results are listed in Table III together with those of related ligand substitution reactions in oxovanadium(IV) complexes.

Kinetic experiments were also carried out at various pressures up to 170 MPa by use of the high-pressure stopped-flow apparatus. Since k_1 and k_2 were difficult to calculate from stopped-flow traces obtained under high pressure, an apparent first-order rate constant k_{app} was determined at various pressures. A plot of $\ln k_{\text{app}}$ *versus* pressure (Fig. 6) shows a straight line yielding the volume of activation as follows: $\Delta V^{\neq} = -0.65 \pm 0.75$ cm^3 mol^{-1} at 20.2 °C. Similar experiments were performed for the replace-
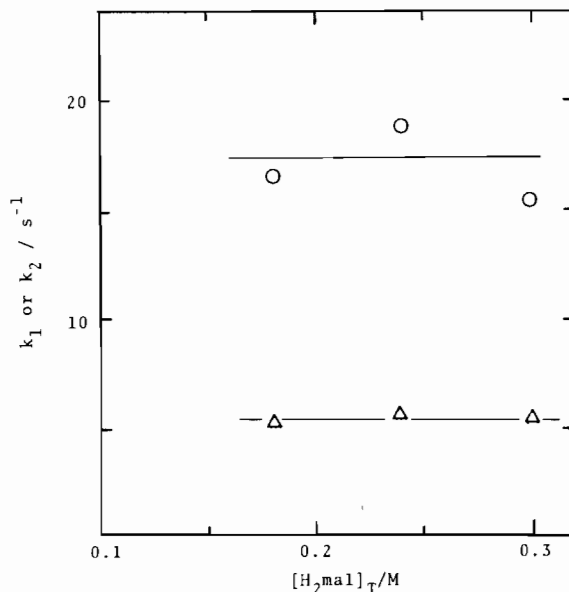

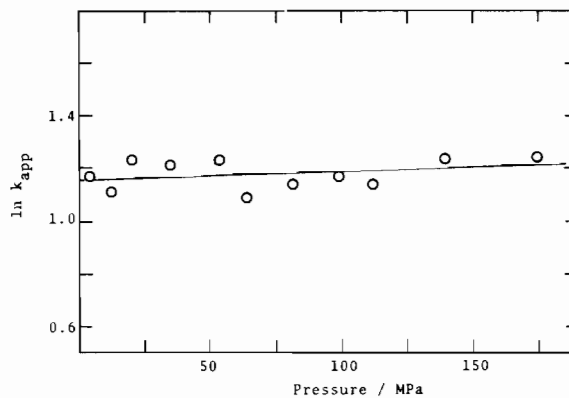Fig. 5. Plots of k_1 or k_2 vs. total malonic acid concentration $[\text{H}_2\text{mal}]_\text{T}$. ○: k_1, △: k_2.

Fig. 6. A plot of $\ln k_{\text{app}}$ vs. pressure. $[\text{VO(mal)}_2]^{2-} = 0.0188$ M, $[\text{Na}_2\text{ox}]_\text{T} = 0.125$ M and pH = 5.26 at 20.2 °C.

TABLE II. Second-order Rate Constants for Malonate Replacement by Oxalate in $[\text{VO(mal)}_2]^{2-}$

Temperature (°C)	$k_{1,\text{ox}}$ (M^{-1} s^{-1})	$k_{2,\text{ox}}$ (M^{-1} s^{-1})
20.5	183	59.2
23.8	247	74.7
24.2	263	74.8
26.4	294	86.3
31.9	377	120

ment of glycinate in VO(gly)_2 by oxalate (eqn. (7)) in order to compare the results in these reactions.
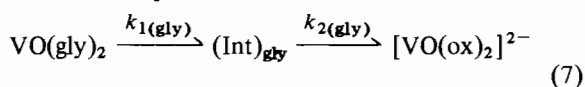
$$\text{VO(gly)}_2 \xrightarrow{k_{1(\text{gly})}} (\text{Int})_{\text{gly}} \xrightarrow{k_{2(\text{gly})}} [\text{VO(ox)}_2]^{2-} \tag{7}$$

TABLE III. Rate Constants and Activation Parameters for Ligand-substitution Reactions in Oxovanadium(IV) Complexes

Reaction	$\Delta H^{\neq}$ (kJ mol^{-1})	$\Delta S^{\neq}$ (J K^{-1} mol^{-1})	Rate constant (20 °C) (mol^{-1} s^{-1})	Reference
$[VO(mal)_2]^{2-} + 2ox^{2-} \rightarrow [VO(ox)_2]^{2-}$				
$k_{1,ox}$	43.5 ± 5.6	-53 ± 19	253	this work
$k_{2,ox}$	43.6 ± 0.5	-62 ± 2	78.5	this work
$VO(gly)_2 + 2ox^{2-} \rightarrow [VO(ox)_2]^{2-}$				
$k_{1(gly)}$	51.2	-55	11.3[a]	8
ox^{2-} exchange in $[VO(ox)_2]^{2-}$	39.8 ± 1.9	-51.6 ± 5.8	1.3×10^3	7
Hox$^-$ exchange in $[VO(ox)_2]^{2-}$	51.0 ± 2.6	-7.6 ± 8.6	2.9×10^3	7

[a]First-order rate constant.
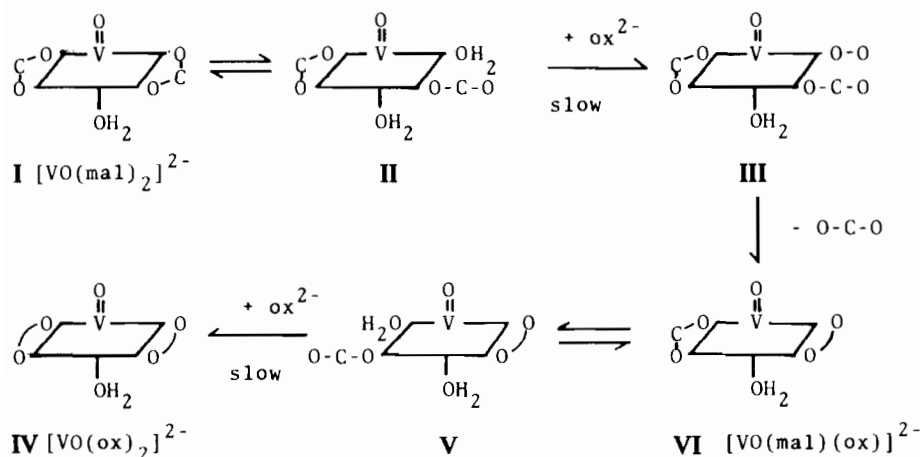

Fig. 7. Proposed mechanism for malonate replacement in $[VO(mal)_2]^{2-}$ by oxalate. Malonate and oxalate are represented by O-C-O and O-O, respectively.

where $k_{1(gly)}$ and $k_{2(gly)}$ are first-order rate constants. The value of $\Delta V^{\neq}$ was determined to be 3.77 ± 1.83 cm^3 mol^{-1} at 19.7 °C.

In a previous paper [8], $(Int)_{gly}$ in eqn. (7) was assigned to a mixed-ligand complex, $[VO(gly)(ox)]^-$, and the rate determining steps were proposed to be the rupture of V–N bonds in $VO(gly)_2$ and $[VO(gly)(ox)]^-$ for $k_{1(gly)}$ and $k_{2(gly)}$ steps, respectively, because both $k_{1(gly)}$ and $k_{2(gly)}$ were independent of free ligand concentrations, $[ox^{2-}]$ and $[Hox^-]$. Similar results were obtained in the present study, *i.e.* the reaction consists of two consecutive steps passing through the mixed-ligand complex. However, unlike the results in the preceding study, both k_1 and k_2 depend linearly on $[ox^{2-}]$ and $[Hox^-]$. From these results, we propose the following mechanism which is illustrated in Fig. 7.

The reaction is initiated by opening one of the chelate rings of mal and thereby forming complex **II**. Complex **II** is attacked by ox^{2-} and/or Hox$^-$ and

forms complex **III**, and then considerably stable complex **IV**. For glycinate replacement by oxalate (eqn. (7)), the rate determining step was the initial ring opening because of the relative inertness of –NH$_2$ in glycinate compared with –COO$^-$, while in the present study, the rate of ring closure (**II** → **I**) of malonate coordinated as a unidentate ligand is expected to be much faster than that of replacement (**II** → **III**) by –COO$^-$ in the outer coordination-sphere. Consequently, the path **II** → **III** controls the rate and k_1 depends linearly on $[ox^{2-}]$ and/or $[Hox^-]$. In the same way, the k_2 step can be explained by the process from **IV** to **VI**. About the same values of activation enthalpy for $k_{1,ox}$ and $k_{2,ox}$ support the similarity in the reaction mechanism of these steps.

The values of k_1 are larger than those of k_2 under all the conditions studied. This is partly accounted for by the fact that the probability of the ring opening of malonate in complex **I** is twice higher than

that in complex **IV**. As complex **IV** is expected to be smaller in size than complex **I**, the electronegativity of complex **IV** seems relatively higher than that of complex **I**. This may also be responsible for the slower exchange rate in complex **IV** than in complex **I** from the standpoint of the electrostatic repulsion between the negative ligands and complexes. As a matter of fact, much smaller values of $k_{1,ox}$ and $k_{2,ox}$ than those of $k_{1,Hox}$ and $k_{2,Hox}$ can be explained by the stronger electrostatic repulsion between ox^{2-} and complex **I** or **IV** as compared with the repulsion between Hox^- and complex **I** or **IV**. Similar results were reported in an earlier paper [7] for oxalate exchange in $[VO(ox)_2]^{2-}$.

The fact that both k_1 and k_2 are independent of $[H_2mal]$ indicates that the reverse processes **IV** → **I** and **VI** → **IV** can be ignored.

The value of -0.65 cm^3 mol^{-1} for activation volume in the malonate replacement (eqn. (1)) is smaller than that of 3.77 cm^3 mol^{-1} for activation volume in the glycinate replacement (eqn. (7)). The results are consistent with the following fact: the rates are dependent on the concentration of free ligand in the malonate replacement, *i.e.* partly associative in the path **II** → **III**, while independent of the concentration of free ligand in the glycinate replacement, where the rupture of the V-glycinate bond is the rate determining step.

Acknowledgements

References

1 K. Wüthrich and R. E. Connick, *Inorg. Chem., 6*, 583 (1987).
2 K. Wüthrich and R. E. Connick, *Inorg. Chem., 7*, 1377 (1968).
3 G. A. Miller and R. E. D. McClung, *J. Chem. Phys., 58*, 4358 (1973).
4 N. S. Angerman and R. B. Jordan, *Inorg. Chem., 8*, 65 (1969).
5 M. Harada, Y. Ikeda, H. Tomiyasu and H. Fukutomi, *Chem. Lett.,* 1195 (1984).
6 H. Tomiyasu, S. Ito and S. Tagami, *Bull. Chem. Soc. Jpn., 47*, 2843 (1974).
7 O. Yokoyama, H. Tomiyasu and G. Gordon, *Inorg. Chem., 21*, 1136 (1982).
8 J.-S. Kim, W.-S. Jung, H. Tomiyasu and H. Fukutomi, *Bull. Chem. Soc. Jpn., 59*, 613 (1986).
9 H. Tomiyasu, K. Dryer and G. Gordon, *Inorg. Chem., 11*, 2409 (1972).
10 M. Nishizawa and K. Saito, *Bull. Chem. Soc. Jpn., 51*, 483 (1978).
11 M. Nishizawa and K. Saito, *Inorg. Chem., 17*, 3676 (1978).
12 M. Nishizawa and K. Saito, *Inorg. Chem., 19*, 2248 (1980).
13 H. Tomiyasu and G. Gordon, *Inorg. Chem., 15*, 870 (1976).
14 K. Kaya, Y. Ikeda and H. Fukutomi, *Bull. Chem. Soc. Jpn., 58*, 2648 (1985).
15 M. Delfini, E. Gaggelli, A. Lepri and G. Valensin, *Inorg. Chim. Acta, 107*, 87 (1985).
16 IUPAC, 'Stability Constants of Metal-Ion Complexes', Part B, 'Organic Ligand', Pergamon, Oxford, 1982.
17 J. H. Espenson, 'Chemical Kinetics and Mechanisms', McGraw-Hill, New York, 1981.